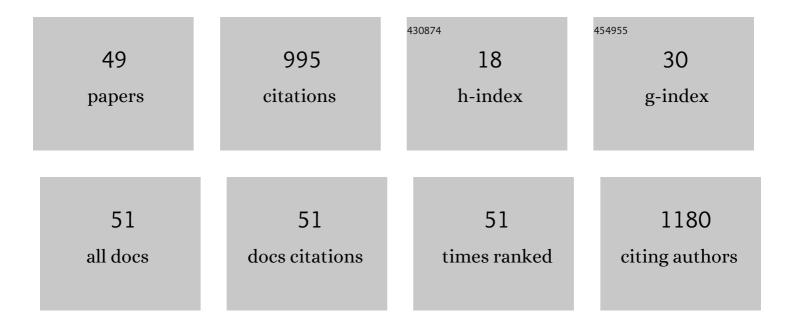
## Xavier Maeder

List of Publications by Year in descending order

Source: https://exaly.com/author-pdf/1713006/publications.pdf Version: 2024-02-01



XAVIED MAEDED

#	Article	IF	CITATIONS
1	Abnormal grain growth in ultrafine grained Ni under high-cycle loading. Scripta Materialia, 2022, 209, 114372.	5.2	9
2	In-situ diffraction based observations of slip near phase boundaries in titanium through micropillar compression. Materials Characterization, 2022, 184, 111695.	4.4	3
3	Phase and microstructure control of electrodeposited Manganese Oxide with enhanced optical properties. Applied Surface Science, 2022, 580, 152289.	6.1	13
4	Anomalous high strain rate compressive behavior of additively manufactured copper micropillars. Applied Materials Today, 2022, 27, 101415.	4.3	5
5	Evolution of deformation twinning mechanisms in magnesium from low to high strain rates. Materials and Design, 2022, 217, 110646.	7.0	8
6	Processability, microstructure and precipitation of a Zr-modified 2618 aluminium alloy fabricated by laser powder bed fusion. Journal of Alloys and Compounds, 2022, 913, 165346.	5.5	11
7	Monolithic and Single-Crystalline Aluminum–Silicon Heterostructures. ACS Applied Materials & Interfaces, 2022, 14, 26238-26244.	8.0	13
8	Dynamic cryo-mechanical properties of additively manufactured nanocrystalline nickel 3D microarchitectures. Materials and Design, 2022, 220, 110836.	7.0	4
9	{		

Xavier Maeder

#	Article	IF	CITATIONS
19	3D HR-EBSD Characterization of the plastic zone around crack tips in tungsten single crystals at the micron scale. Acta Materialia, 2020, 200, 211-222.	7.9	30
20	Synthesis of model Al-Al2O3 multilayer systems with monolayer oxide thickness control by circumventing native oxidation. Thin Solid Films, 2020, 711, 138287.	1.8	14
21	Crystal Structure Evolution, Microstructure Formation, and Properties of Mechanically Alloyed Ultrafine-Grained Ti-Zr-Nb Alloys at 36а‰爾â‰戽0 (at. %). Materials, 2020, 13, 587.	2.9	7
22	A computational and experimental comparison on the nucleation of fatigue cracks in statistical volume elements. International Journal of Fatigue, 2020, 137, 105633.	5.7	14
23	Dual-templated electrodeposition and characterization of regular metallic foam based microarchitectures. Applied Materials Today, 2020, 20, 100667.	4.3	5
24	A self-aligning microtensile setup: Application to single-crystal GaAs microscale tension–compression asymmetry. Journal of Materials Research, 2019, 34, 2517-2534.	2.6	18
25	Grain refinement mechanism of nickel-based superalloy by severe plastic deformation - Mechanical machining case. Acta Materialia, 2019, 180, 2-14.	7.9	103
26	The effect of Î'-hydride on the micromechanical deformation of a Zr alloy studied by in situ high angular resolution electron backscatter diffraction. Scripta Materialia, 2019, 173, 101-105.	5.2	18
27	Pulsed current-voltage electrodeposition of stoichiometric Bi2Te3 nanowires and their crystallographic characterization by transmission electron backscatter diffraction. Science and Technology of Advanced Materials, 2019, 20, 1022-1030.	6.1	7
28	Mechanical Anisotropy Investigated in the Complex SLMâ€Processed Sc―and Zrâ€Modified Al–Mg Alloy Microstructure. Advanced Engineering Materials, 2019, 21, 1801113.	3.5	26
29	The role of Î <sup>2</sup> -titanium ligaments in the deformation of dual phase titanium alloys. Materials Science & Engineering A: Structural Materials: Properties, Microstructure and Processing, 2019, 746, 394-405.	5.6	22
30	Microstructural and micromechanical investigations of surface strengthening mechanisms induced by repeated impacts on pure iron. Materials and Design, 2018, 147, 56-64.	7.0	21
31	Interplay of stresses, plasticity at crack tips and small sample dimensions revealed by in-situ microcantilever tests in tungsten. Materials Science & Engineering A: Structural Materials: Properties, Microstructure and Processing, 2018, 710, 400-412.	5.6	15
32	In situ micromechanical testing of tungsten micro-cantilevers using HR-EBSD for the assessment of deformation evolution. Materials and Design, 2017, 117, 265-266.	7.0	23
33	Microstructure and mechanical properties of near net shaped aluminium/alumina nanocomposites fabricated by powder metallurgy. Journal of Alloys and Compounds, 2017, 714, 133-143.	5.5	43
34	Elevated temperature, micro-compression transient plasticity tests on nanocrystalline Palladium-Gold: Probing activation parameters at the lower limit of crystallinity. Acta Materialia, 2017, 129, 124-137.	7.9	13
35	Electrodeposition of dilute Ni-W alloy with enhanced thermal stability: Accessing nanotwinned to nanocrystalline microstructures. Materials Today Communications, 2017, 12, 63-71.	1.9	14
36	Reversible, high temperature softening of plasma-nitrided hot-working steel studied using in situ micro-pillar compression. Materials Science & Engineering A: Structural Materials: Properties, Microstructure and Processing, 2017, 680, 433-436.	5.6	4

#	Article	IF	CITATIONS
37	Annealing-Based Electrical Tuning of Cobalt–Carbon Deposits Grown by Focused-Electron-Beam-Induced Deposition. ACS Applied Materials & Interfaces, 2016, 8, 32496-32503.	8.0	28
38	Microstructure, Mechanical, and Impression Creep Properties of AlMg5–0.5 vol% Al <sub>2</sub> O <sub>3</sub> Nanocomposites. Advanced Engineering Materials, 2016, 18, 1958-1966.	3.5	8
39	Silicon etch with chromium ions generated by a filtered or non-filtered cathodic arc discharge. Science and Technology of Advanced Materials, 2016, 17, 20-28.	6.1	1
40	Influence of microstructure and strengthening mechanism of AlMg5–Al 2 O 3 nanocomposites prepared via spark plasma sintering. Materials and Design, 2016, 95, 534-544.	7.0	49
41	Nanomechanical investigation of thin-film electroceramic/metal-organic framework multilayers. Applied Physics Letters, 2015, 107, .	3.3	9
42	Comparison of In Situ Micromechanical Strain-Rate Sensitivity Measurement Techniques. Jom, 2015, 67, 1684-1693.	1.9	35
43	Complex vein systems as a data source in tectonics: An example from the Ugab Valley, NW Namibia. Journal of Structural Geology, 2014, 62, 125-140.	2.3	10
44	Plasticity and fracture of sapphire at room temperature: Load-controlled microcompression of four different orientations. Ceramics International, 2014, 40, 2083-2090.	4.8	58
45	Crystallographic Services and Technology Support for Industry. Chimia, 2014, 68, 14-18.	0.6	Ο
46	Pinch-and-swell structure and shear zones in viscoplastic layers. Journal of Structural Geology, 2012, 37, 75-88.	2.3	49
47	Synthesis Mechanisms of Organized Gold Nanoparticles: Influence of Annealing Temperature and Atmosphere. Crystal Growth and Design, 2010, 10, 587-596.	3.0	122
48	Modelling of segment structures: Boudins, bone-boudins, mullions and related single- and multiphase deformation features. Journal of Structural Geology, 2009, 31, 817-830.	2.3	20
49	Flame foliation: Evidence for a schistosity formed normal to the extension direction. Journal of Structural Geology, 2007, 29, 378-384.	2.3	3